

Downscaling metawebs: propagation of uncertainties in species distribution and interaction probability

Gabriel Dansereau^{1,2,‡} Ceres Barros³ Timothée Poisot^{1,2}

¹ Université de Montréal ² Québec Centre for Biodiversity Sciences ³ University of British Columbia

‡ Equal contributions

Correspondance to:

Gabriel Dansereau — gabriel.dansereau@umontreal.ca

1 Introduction

2 Sampling species interactions and ecological networks in repeated locations in space and time is a challenging
3 task (Jordano 2016). Most studies on food webs have previously focused on local webs limited in size and
4 extent, and are rarely replicated in space and time (Mestre *et al.* 2022). Interactions can show important
5 variations in space (Poisot *et al.* 2015), yet available network data also show important geographical bias,
6 limiting our ability to answer questions in many biomes and over broad spatial extents (Poisot *et al.* 2021).
7 Moreover, global network monitoring is insufficient to properly describe and understand how ecosystems are
8 reacting to global change (**Windsor2023UsiEco?**). Predictive approaches are increasingly used to predict
9 species interactions (Morales-Castilla *et al.* 2015; e.g. Desjardins-Proulx *et al.* 2017) and can handle limited
10 data to circumvent data scarcity (Strydom *et al.* 2021), but they are rarely used to make explicitly spatial
11 predictions. As a result, there have been repeated calls for globally distributed interaction and network data and
12 repeated samplings in time and space (Poisot *et al.* 2021; Mestre *et al.* 2022; **Windsor2023UsiEco?**).

13 The metaweb is an increasingly used concept to address the issue of data scarcity, and it further holds potential
14 to analyse networks at large spatial extents. A metaweb contains all the possible interactions between the
15 species found in a given regional species pool (Dunne 2006). Studies are now directly focused on assembling
16 metawebs for various taxa through extensive literature surveys (Maiorano *et al.* 2020) or using predictive tools
17 (Strydom *et al.* 2022a). These new data sources have allowed studying network structures in novel ways, for
18 instance, assessing changes in food web structure across space (Braga *et al.* 2019), the scaling of network area
19 relationships (Galiana *et al.* 2021), or how sampling effort affects measured network structure (McLeod *et al.*
20 2021). A key element that emerged from these studies is that the structure of empirical food webs is inherited
21 from the metaweb with little influence from habitat and dynamical constraints (Saravia *et al.* 2022). This makes
22 the metaweb the core goal of predictive network ecology (Strydom *et al.* 2022b), i.e. the first approximation of
23 networks in space we should aim for. This is not the same as using interactions to improve predictions of
24 species distributions as recent studies have done (Moens *et al.* 2022; for example, Poggiato *et al.* 2022; Lucas *et*
25 *al.* 2023), answering long-standing calls to include interactions within such models (Wisz *et al.* 2013). Instead,
26 predicting networks in space is a different task and it serves a different goal, focusing first on the distribution of
27 networks and its drivers rather than on the distribution of species.

28 Two network aspects are essential to develop a proper spatial perspective: the influence from the metaweb and
29 the probabilistic representation. First, networks are local realizations of a regional metaweb (Poisot *et al.* 2012,

2015) whose structure they inherit (Saravia *et al.* 2022). Therefore, establishing or predicting the metaweb should be the first target for systems where we lack information about local realizations (Strydom *et al.* 2022b). Second, to account for their variability in space, interactions must be seen as probabilistic events (Poisot *et al.* 2016). In contrast, many studies assume interactions are binary events, whether at the interaction, network or metaweb level (Gaüzère *et al.* 2022; Mendoza & Araujo 2022). However, a probabilistic view can additionally allow propagating uncertainty, which can play a key role in evaluating the quality of the predictions. Moreover, assessing model uncertainty would enable us to assess to which degree we should trust our predictions and to identify what to do to improve the current knowledge. For instance, we could locate where our knowledge and models are the most uncertain and determine new sampling sites or areas where repeated sampling is necessary. Explicit spatial predictions such as downscaled metaweb predictions are essential as they will allow comparisons with extant work for species communities. These comparisons are relevant as they may go in unexpected directions and highlight new elements regarding network biogeography. For instance, Frelat *et al.* (2022) found a strong spatial coupling between community composition and food web structure but a temporal mismatch depending on the spatial scale. Poisot *et al.* (2017) found that interaction uniqueness captures more composition variability than community uniqueness and that sites with exceptional compositions might not be the same for networks and communities. Spatialized network data will allow these comparisons and allow identifying important conservation targets for networks and whether they differ geographically from areas currently prioritized for biodiversity conservation.

Here, we present a method to downscale a metaweb in space by spatially reconstructing local instances of a probabilistic metaweb of Canadian mammals. We explore how the spatial structure of the downscaled metaweb varies in space and how the uncertainty of interactions can be made spatially explicit. We further show that the downscaled metaweb can highlight important biodiversity areas and bring novel ecological insights compared to traditional community measures like species richness.

Methods

Fig. 1 shows a conceptual overview of the methodological steps leading to the downscaled metaweb. The components were grouped as non-spatial and spatial inputs, localized steps (divided into single-species-level, two-species-level, and network-level steps), and the final downscaled and spatialized metaweb. Throughout these steps, we highlight the importance of presenting the uncertainty of interactions and of their distribution in

58 space. We argue that this requires adopting a probabilistic view and incorporating variation between scales.

59 [Figure 1 about here.]

60 **Non-spatial inputs**

61 The main source of interaction data was the metaweb for Canadian mammals from Strydom *et al.* (2022a),
62 which is a-spatial, i.e., it represents interactions between mammals that can occur anywhere in Canada. The
63 species list for the Canadian metaweb was extracted from the International Union for the Conservation of
64 Nature (IUCN) checklist (Strydom *et al.* 2022a). Briefly, the metaweb was developed using graph embedding
65 and phylogenetic transfer learning based on the metaweb of European mammals, which is itself based on a
66 comprehensive survey of interactions reported in the scientific literature (Maiorano *et al.* 2020). The Canadian
67 metaweb is probabilistic, which has the advantage of reflecting the likelihood of an interaction taking place
68 given the phylogenetic and trait match between two species. This allows incorporating interaction variability
69 between species (i.e., taking into account that two species may not always interact whenever or wherever they
70 occur); however, we highlight that other factors beyond trait and phylogenetic matching (e.g., population
71 densities) will also contribute to observed interaction probabilities.

72 **Spatial inputs**

73 The downscaling of the metaweb involved combining it with species occurrence and environmental data. First,
74 we extracted species occurrences from the Global Biodiversity Information Facility (GBIF; www.gbif.org) for
75 the Canadian mammals after reconciling species names between the Canadian metaweb and GBIF using the
76 GBIF Backbone Taxonomy (GBIF Secretariat 2021). Doing so, we removed potential duplicates where species
77 listed in the Canadian metaweb are considered as a single entity by GBIF. We collected occurrences for our
78 species list (159 species) using the GBIF download API on October 21st 2022 (GBIF.org 2022). We restricted
79 our query to occurrences with coordinates between longitudes 175°W to 45°W and latitudes 10°N to 90°N. This
80 was meant to collect training data covering a broader range than our prediction target (Canada only) and include
81 observations in similar environments. Then, since GBIF observations represent presence-only data and most
82 predictive models require absence data, we generated pseudo-absence data using the surface range envelope
83 method available in `SimpleSDMLayers.jl` (Dansereau & Poisot 2021). This method generates pseudo-absences

84 by selecting random non-observed sites within the spatial range delimited by the presence data (Barbet-Massin
85 *et al.* 2012).

86 We used species distribution models (SDMs, Guisan & Thuiller 2005) to project Canadian mammal habitat
87 suitability across the country, which we treated as information on potential distribution. For each species, we
88 related occurrences and pseudo-absences with 19 bioclimatic variables from CHELSA (Karger *et al.* 2017) and
89 12 consensus land-cover variables from EarthEnv (Tuanmu & Jetz 2014). The CHELSA bioclimatic variables
90 (*bio1-bio19*) represent various measures of temperature and precipitation (e.g., annual averages, monthly
91 maximum or minimum, seasonality) and are available for land areas across the globe. We used the most recent
92 version, the CHELSA v2.1 dataset (Karger *et al.* 2021), and subsetting it to land surfaces only using the
93 CHELSA v1.2 (Karger *et al.* 2018), which does not cover open water. The EarthEnv land-cover variables
94 represent classes such as Evergreen broadleaf trees, Cultivated and managed vegetation, Urban/Built-up, and
95 Open Water. Values range between 0 and 100 and represent the consensus prevalence of each class in
96 percentage within a pixel (hereafter considered as sites). We coarsened both the CHELSA and EarthEnv data
97 from their original 30 arc-second resolution to a 2.5 arc-minute one (around 4.5 km at the Equator) using
98 GDAL (GDAL/OGR contributors 2021). This resolution compromised capturing both local variations and
99 broad scale patterns, while limiting computation costs to a manageable level as memory requirements increase
100 rapidly with spatial resolution.

101 Our selection criteria for choosing an SDM algorithm was to have a method that generated probabilistic results
102 (similar to **Gravel2019BriElt?**), including both a probability of occurrence for a species in a specific site and
103 the uncertainty associated with the prediction. These were crucial to obtaining a probabilistic version of the
104 metaweb as they were used to create spatial variations in the localized interaction probabilities (see next
105 section). One suitable method for this is Gradient Boosted Trees with a Gaussian maximum likelihood from the
106 `EvoTrees.jl` *Julia* package (<https://github.com/Evovest/EvoTrees.jl>). This method returns a prediction for
107 every site with an average value and a standard deviation, which we used as a measure of uncertainty to build a
108 Normal distribution for the probability of occurrence of a given species at all sites (represented as probability
109 distributions on Fig. 1). We trained models across the extent chosen for occurrences (longitudes 175°W to
110 45°W and latitudes 10°N to 90°N), then predicted species distributions only for Canada. We used the 2021
111 Census Boundary Files from Statistics Canada (Statistics Canada 2022) to set the boundaries for our
112 predictions, which gave us 970,698 sites in total.

Localized steps: Building site-level instances of the metaweb

The next part of the method was the localized steps which produce local metawebs for every site. This component was divided into single-species, two-species, and network-level steps (*Localized steps* box on Fig. 1).

The single-species steps represented four possible ways to account for uncertainty in the species distributions and bring variation to the spatial metaweb. We explored four different options to select a value ($P(\textit{occurrence})$; Fig. 1) from the occurrence distributions obtained in the previous steps (Inputs section): 1) taking the mean from the distribution as the probability of occurrence (option 1 on Fig. 1); 2) converting the mean value to a binary one using a specific threshold per species (option 2); 3) sampling a random value within the Normal distribution (option 3); or 4) converting a random value into a binary result (option 4, using a separate draw from option 3 and the same threshold as in option 2). The threshold (τ on Fig. 1) used was the value that maximized Youden's J informedness statistic (Youden 1950), the same metric used by Strydom *et al.* (2022a) at an intermediate step while building the metaweb. The four sampling options were intended to explore how uncertainty and variation in the species distributions can affect the metaweb result. We expected thresholding to have a more pronounced effect on network structure as it should reduce the number of links by removing many of the rare interactions (Poisot *et al.* 2016). Meanwhile, we expected random sampling to create spatial heterogeneity compared to the mean probabilities, as including some extreme values should confound the potential effects of environmental gradients. We chose option 1 as the default to present results as it is intuitive and essentially represents the result of a probabilistic SDM (as in Gravel2019BriElt?).

Next, the two-species steps were aimed at assigning a probability of observing an interaction between two species in a given site. For each species pair, we multiplied the product of the two species' occurrence probabilities ($P(\textit{co-occurrence})$; Fig. 1) (obtained using the one of the sampling options above) by their interaction probability in the Canadian metaweb. For cases where species in the Canadian metaweb were considered as the same species by the GBIF Backbone Taxonomy (the reconciliation step mentioned earlier), we used the highest interaction probabilities involving the duplicated species.

The network-level steps then created the probabilistic metaweb for the site. We assembled all the local interaction probabilities (from the two-species steps) into a probabilistic network (Poisot *et al.* 2016). We then sampled several random network realizations to represent the potential local realization process (Poisot *et al.* 2015). This resulted in a distribution of localized networks, which we averaged over the number of simulations to obtain a single probabilistic network for the site.

142 **Outputs: The downscaled metaweb**

143 The final output of our method was the downscaled metaweb, which contains a localized probabilistic metaweb
144 in every site across the study area (Outputs box on Fig. 1). A metaweb essentially serves to set an upper bound
145 on the potential interactions (Strydom *et al.* 2022b); therefore, the downscaled metaweb is a refined upper
146 boundary at the local scale taking into account co-occurrences. It is still potential in nature and differs from a
147 local realization, from which it should have a different structure. Nonetheless, from the downscaled metaweb
148 we can create maps of network properties (e.g. number of links, connectance) measured on the local
149 probabilities, display their spatial distribution, and compute some traditional community-level measures such as
150 species richness. We can also calculate the uncertainty associated with the network and community
151 measurements and compare their spatial distribution (see Supplementary Material). We computed expected
152 metrics on probabilistic networks following Poisot *et al.* (2016; see Gravel2019BriElt? for a similar example).

153 **Analyses of results by ecoregions**

154 Since both species composition and network summary values display a high spatial variation and complex
155 patterns, we simplified the representation of their distribution by grouping sites by ecoregion, as species and
156 interaction composition have been shown to differ between ecoregions across large spatial scales (Martins *et al.*
157 2022). To do so, we rasterized the Canadian subset of the global map of ecoregions from Dinerstein *et al.*
158 (2017; also used by Martins *et al.* 2022), which resulted in 44 different ecoregions. For every measure we
159 report (e.g. species richness, number of links), we calculated the median site value for each ecoregion. We also
160 measured within-ecoregion variation as the 89% interquantile range of the site values in each ecoregion
161 (threshold chosen to avoid confusion with conventional significance tests; McElreath 2020).

162 **Analyses of ecological uniqueness**

163 We compared the compositional uniqueness of the networks and the communities to assess whether they
164 indicated areas of exceptional composition. We measured uniqueness using the local contributions to beta
165 diversity (LCBD, Legendre & De Cáceres 2013), which identify sites with exceptional composition by
166 quantifying how much one site contributes to the total variance in the community composition. While many
167 studies used LCBD values to evaluate uniqueness on local scales or few study sites (for example, da Silva &
168 Hernández 2014; Heino & Grönroos 2017), recent studies used the measure on predicted species compositions

over broad spatial extents and a large number of sites (Vasconcelos *et al.* 2018; Dansereau *et al.* 2022). LCBD values can also be used to measure uniqueness for networks by computing the values over the adjacency matrix, which has been shown to capture more unique sites and uniqueness variability than through species composition (Poisot *et al.* 2017). Here, we measured and compared the uniqueness of our localized community and network predictions. For species composition, we assembled a site-by-species community matrix with the probability of occurrence at every site from the species distribution models. For network composition, we assembled a site-by-interaction matrix with the localized interaction values from the spatial probabilistic metaweb. We applied the Hellinger transformation on both matrices and computed the LCBD values from the total variance in the matrices (Legendre & De Cáceres 2013). High LCBD values indicate a high contribution to the overall variance and a unique species or interaction composition compared to other sites. Since values themselves are very low given our high number of sites (as in Dansereau *et al.* 2022), what matters primarily is the magnitude of the difference between the sites. Given this, we divided values by the maximum value in each matrix (species or network) and suggest that these should be viewed as relative contributions compared to the highest observed contribution. As with other measures, we then summarized the local uniqueness values by ecoregion by taking the median LCBD value and measuring the 89% interquantile range within all ecoregions.

We used *Julia* v1.9.0 (Bezanson *et al.* 2017) to implement all our analyses. We used packages `GBIF.jl` (Dansereau & Poisot 2021) to reconcile species names using the GBIF Backbone Taxonomy, `SpeciesDistributionToolkit.jl` to handle raster layers and species occurrences, `EcologicalNetworks.jl` (Poisot *et al.* 2019) to analyse network and metaweb structure, and `Makie.jl` (Danisch & Krumbiegel 2021) to produce figures. Our data sources (CHELSA, EarthEnv, Ecoregions) were all unprojected and we did not use a projection in our analyses, but we displayed the results using a Lambert conformal conic projection more appropriate for Canada using `GeoMakie.jl`. All the code used to implement our analyses is available on GitHub (<https://github.com/PoisotLab/SpatialProbabilisticMetaweb>) and includes instructions on how to run a smaller example at a coarser resolution. Note that running our analyses at full scale is resource and memory intensive and required the use of compute clusters provided by Calcul Québec and the Digital Research Alliance of Canada.

Results

Our method allowed us to display the spatial distribution of ecoregion-level community measures (here expected species richness) and network measures (expected number of links; Fig. 2). We highlight that the community and network-level measures presented here are not actual predictions of the measure itself (e.g., we do not present a prediction of actual species richness at each location). Instead, they are the reflection of these metrics from the localized predictions of the communities and networks obtained from the downscaling of the metaweb, then summarized for the ecoregions (median value). Expected ecoregion richness (Fig. 2A) and expected number of links (Fig. 2B) displayed similar distributions with a latitudinal gradient and higher values in the south. However, within-ecoregion variability was distributed differently, as some ecoregions along the coasts displayed higher interquantile ranges while ecoregions around the southern border displayed narrower ones (Fig. 2C-D). All results shown are based on the first sampling strategy (option 1) mentioned in the Localized steps section, where species occurrence probabilities were taken as the mean value of the distribution (results for other sampling strategies are discussed in Supplementary Material).

[Figure 2 about here.]

Direct comparison of the spatial distributions of species richness and expected number of links showed some areas with mismatches, both regarding the median estimates and regarding the within-ecoregion variability (Fig. 3). Median values for the ecoregions showed a similar bivariate distribution with ecoregions in the south mostly displaying high species richness and a high number of links (Fig. 3A). The northernmost ecoregions (Canadian High Arctic Tundra and Davis Highlands Tundra) displayed higher richness (based on the quantile rank) compared to the number of links. Inversely, ecoregions further south (Canadian Low Arctic Tundra, Northern Canadian Shield Taiga, Southern Hudson Bay Taiga) ranked higher for the number of links than for species richness. On the other hand, within-ecoregion variability showed different bivariate relationships and a less constant latitudinal gradient (Fig. 3B). This indicates that richness and links do not co-vary completely (i.e. their variability is not closely connected) although they may show similar distributions for median values.

[Figure 3 about here.]

Our results also indicate a mismatch between the uniqueness of communities and networks (Fig. 4). Uniqueness was higher mostly in the north and along the south border for communities, but only in the north for networks

(Fig. 4A-B). Consequently, ecoregions with both unique community composition and unique network composition were mostly in the north (Fig. 4C). Meanwhile, some areas were unique for one element but not the other. For instance, the New England-Acadian forests ecoregion (south-east, near 70°W and 48°N) had a highly unique species composition but a more common network composition (Fig. 4C). Opposite areas with unique network compositions only were observed at higher between latitudes 52°N and 70°N (Eastern Canadian Shield Taiga, Northern Canadian Shield Taiga, Canadian Low Arctic Tundra). Also, network uniqueness values for ecoregions spanned a narrower range between the 44 ecoregions than species LCBBD values (Fig. 4D, left). Within-ecoregion variation was also lower for network values with generally lower 89% interquantile ranges among the site-level LCBBD values (Fig. 4D, right). Moreover, mismatched sites (unique for only one element) formed two distinct groups when evaluating the relationship between species richness and the number of links (see Supplementary Material). The areas only unique for their species composition had both a high richness and number of links. On the other hand, the sites only unique for their networks had both lower richness and a lower number of links, although they were not the sites with the lowest values for both.

[Figure 4 about here.]

Discussion

Our approach presents a way to downscale a metaweb and produce localized predictions using probabilistic networks as inputs and outputs and incorporating uncertainty, as called for by Strydom *et al.* (2022b). It gives us an idea of what local metawebs or networks could look like in space, given the species distributions and their variability, as well as the uncertainty around the interactions. We also provide the first spatial representation of the metaweb of Canadian mammals (Strydom *et al.* 2022a) and a probabilistic equivalent to how the European tetrapod metaweb (Maiorano *et al.* 2020) was used to predict localized networks in Europe (Braga *et al.* 2019; O'Connor *et al.* 2020; Galiana *et al.* 2021; Gaüzère *et al.* 2022; Botella *et al.* 2023). Therefore, our approach could open similar possibilities of investigations in North America with food webs of Canadian mammals, for instance on the structure of food webs over space (Braga *et al.* 2019) and on the effect of land-use intensification on food webs (Botella *et al.* 2023). Interesting research areas could include assessing climate change impacts on network structure or investigating linkages between network structure and stability. Moreover, since our approach is probabilistic, it does not assume species interact whenever they co-occur, and incorporates variability based on environmental conditions, which could lead to different results by introducing

250 a different association between species richness and network properties. Galiana *et al.* (2021) found that species
251 richness had a large explanatory power over network properties but mentioned it could potentially be due to
252 interactions between species being fixed in space. Here, we found mismatches in the distribution of species
253 richness and interactions, and especially regarding their within-ecoregion variability (Fig. 3), highlighting that
254 interactions might vary differently than species distributions in space. Network measures (links on Fig. 3A)
255 were also lower in the north, contrarily to previous studies (e.g. connectance higher in the north, Braga *et al.*
256 2019; Galiana *et al.* 2021).

257 Our LCBD and uniqueness results highlighted that areas with unique network composition might differ from
258 sites with unique species composition. In other words, the joint distribution of community and network
259 uniqueness highlights different diversity hotspots. Poisot *et al.* (2017) showed a similar result with host-parasite
260 communities of rodents and ecto-fleas. Our results further show how these differences could be distributed
261 across ecoregions and a broad spatial extent. Areas unique for only one element (species or network
262 composition) differed in their combination of species richness and number of links (supplementary material),
263 with species-unique sites displaying high values of both measures and network-unique sites displaying low
264 values. Moreover, LCBD scores essentially highlight variability hotspots and are a measure of the variance of
265 community or network structure. Here they also serve as an inter-ecoregion variation measure which can be
266 compared to the within-ecoregion variation highlighted by the interquartile ranges. The narrower range of
267 values for network LCBD values and the lower IQR values indicate that both the inter-ecoregion and
268 within-ecoregion variation are lower for network than for species (Fig. 4). Additionally, higher values for
269 network LCBD also indicate that most ecoregions can hold ecologically unique sites.

- Barbet-Massin, M., Jiguet, F., Albert, C.H. & Thuiller, W. (2012). [Selecting pseudo-absences for species distribution models: How, where and how many?](#) *Methods in Ecology and Evolution*, 3, 327–338.
- Bezanson, J., Edelman, A., Karpinski, S. & Shah, V.B. (2017). [Julia: A fresh approach to numerical computing.](#) *SIAM Review*, 59, 65–98.
- Botella, C., Gaüzère, P., O'Connor, L., Ohlmann, M., Renaud, J., Dou, Y., *et al.* (2023). [Land-use intensity influences European tetrapod food-webs](#) (Preprint). Preprints.
- Braga, J., Pollock, L.J., Barros, C., Galiana, N., Montoya, J.M., Gravel, D., *et al.* (2019). [Spatial analyses of multi-trophic terrestrial vertebrate assemblages in Europe.](#) *Global Ecology and Biogeography*, 28, 1636–1648.
- da Silva, P.G. & Hernández, M.I.M. (2014). [Local and regional effects on community structure of dung beetles in a mainland-island scenario.](#) *PLOS ONE*, 9, e111883.
- Danisch, S. & Krumbiegel, J. (2021). [Makie.jl: Flexible high-performance data visualization for Julia.](#) *Journal of Open Source Software*, 6, 3349.
- Dansereau, G., Legendre, P. & Poisot, T. (2022). [Evaluating ecological uniqueness over broad spatial extents using species distribution modelling.](#) *Oikos*, 2022, e09063.
- Dansereau, G. & Poisot, T. (2021). [SimpleSDMLayers.jl and GBIF.jl: A framework for species distribution modeling in Julia.](#) *Journal of Open Source Software*, 6, 2872.
- Desjardins-Proulx, P., Laigle, I., Poisot, T. & Gravel, D. (2017). [Ecological interactions and the Netflix problem.](#) *PeerJ*, 5, e3644.
- Dinerstein, E., Olson, D., Joshi, A., Vynne, C., Burgess, N.D., Wikramanayake, E., *et al.* (2017). [An Ecoregion-Based Approach to Protecting Half the Terrestrial Realm.](#) *BioScience*, 67, 534–545.
- Dunne, J. (2006). The network structure of food webs. In: *Ecological Networks: Linking Structure to Dynamics in Food Webs*. pp. 27–86.
- Frelat, R., Kortsch, S., Kröncke, I., Neumann, H., Nordström, M.C., Olivier, P.E.N., *et al.* (2022). [Food web structure and community composition: A comparison across space and time in the North Sea.](#) *Ecography*, 2022.

297 Galiana, N., Barros, C., Braga, J., Ficetola, G.F., Maiorano, L., Thuiller, W., *et al.* (2021). [The spatial scaling of](#)
 298 [food web structure across European biogeographical regions](#). *Ecography*, 44, 653–664.

299 Gaüzère, P., O'Connor, L., Botella, C., Poggiato, G., Münkemüller, T., Pollock, L.J., *et al.* (2022). [The diversity](#)
 300 [of biotic interactions complements functional and phylogenetic facets of biodiversity](#). *Current Biology*.

301 GBIF Secretariat. (2021). [GBIF Backbone Taxonomy](#).

302 GBIF.org. (2022). [GBIF occurrence download](#).

303 GDAL/OGR contributors. (2021). *GDAL/OGR geospatial data abstraction software library*. Manual. Open
 304 Source Geospatial Foundation.

305 Guisan, A. & Thuiller, W. (2005). [Predicting species distribution: Offering more than simple habitat models](#).
 306 *Ecology Letters*, 8, 993–1009.

307 Heino, J. & Grönroos, M. (2017). [Exploring species and site contributions to beta diversity in stream insect](#)
 308 [assemblages](#). *Oecologia*, 183, 151–160.

309 Jordano, P. (2016). [Sampling networks of ecological interactions](#). *Functional Ecology*, 30, 1883–1893.

310 Karger, D.N., Conrad, O., Böhner, J., Kawohl, T., Kreft, H., Soria-Auza, R.W., *et al.* (2017). [Climatologies at](#)
 311 [high resolution for the earth's land surface areas](#). *Scientific Data*, 4, 170122.

312 Karger, D.N., Conrad, O., Böhner, J., Kawohl, T., Kreft, H., Soria-Auza, R.W., *et al.* (2018). [Data from:](#)
 313 [Climatologies at high resolution for the earth's land surface areas](#).

314 Karger, D.N., Conrad, O., Böhner, J., Kawohl, T., Kreft, H., Soria-Auza, R.W., *et al.* (2021). [Climatologies at](#)
 315 [high resolution for the earth's land surface areas](#).

316 Legendre, P. & De Cáceres, M. (2013). [Beta diversity as the variance of community data: Dissimilarity](#)
 317 [coefficients and partitioning](#). *Ecology Letters*, 16, 951–963.

318 Lucas, P., Thuiller, W., Talluto, M., Polaina, E., Albrecht, J., Selva, N., *et al.* (2023). [Including biotic](#)
 319 [interactions in species distribution models improves the understanding of species niche: A case of study](#)
 320 [with the brown bear in Europe](#).

321 Maiorano, L., Montemaggiore, A., Ficetola, G.F., O'Connor, L. & Thuiller, W. (2020). [TETRA-EU 1.0: A](#)
 322 [species-level trophic metaweb of European tetrapods](#). *Global Ecology and Biogeography*, 29, 1452–1457.

323 Martins, L.P., Stouffer, D.B., Blendinger, P.G., Böhning-Gaese, K., Buitrón-Jurado, G., Correia, M., *et al.*

(2022). [Global and regional ecological boundaries explain abrupt spatial discontinuities in avian frugivory interactions](#). *Nature Communications*, 13, 6943.

McElreath, R. (2020). *Statistical rethinking: A bayesian course with examples in R and Stan*. Second. Chapman and Hall/CRC, New York.

McLeod, A., Leroux, S.J., Gravel, D., Chu, C., Cirtwill, A.R., Fortin, M.-J., *et al.* (2021). [Sampling and asymptotic network properties of spatial multi-trophic networks](#). *Oikos*, 130, 2250–2259.

Mendoza, M. & Araujo, M.B. (2022). [Biogeography of bird and mammal trophic structures](#). *Ecography*, 2022, e06289.

Mestre, F., Gravel, D., García-Callejas, D., Pinto-Cruz, C., Matias, M.G. & Araújo, M.B. (2022). [Disentangling food-web environment relationships: A review with guidelines](#). *Basic and Applied Ecology*, 61, 102–115.

Moens, M., Biesmeijer, J., Huang, E., Vereecken, N. & Marshall, L. (2022). [The importance of biotic interactions in distribution models depends on the type of ecological relations, spatial scale and range](#).

Morales-Castilla, I., Matias, M.G., Gravel, D. & Araújo, M.B. (2015). [Inferring biotic interactions from proxies](#). *Trends in Ecology & Evolution*, 30, 347–356.

O'Connor, L.M.J., Pollock, L.J., Braga, J., Ficetola, G.F., Maiorano, L., Martinez-Almoyna, C., *et al.* (2020). [Unveiling the food webs of tetrapods across Europe through the prism of the Eltonian niche](#). *Journal of Biogeography*, 47, 181–192.

Poggiato, G., Andréoletti, J., Shirley, L. & Thuiller, W. (2022). [Integrating food webs in species distribution models improves ecological niche estimation and predictions](#) (Preprint). Preprints.

Poisot, T., Bélisle, Z., Hoebeke, L., Stock, M. & Szefer, P. (2019). [EcologicalNetworks.jl: Analysing ecological networks of species interactions](#). *Ecography*, 42, 1850–1861.

Poisot, T., Bergeron, G., Cazelles, K., Dallas, T., Gravel, D., MacDonald, A., *et al.* (2021). [Global knowledge gaps in species interaction networks data](#). *Journal of Biogeography*, 48, 1552–1563.

Poisot, T., Canard, E., Mouillot, D., Mouquet, N. & Gravel, D. (2012). [The dissimilarity of species interaction networks](#). *Ecology Letters*, 15, 1353–1361.

Poisot, T., Cirtwill, A.R., Cazelles, K., Gravel, D., Fortin, M.-J. & Stouffer, D.B. (2016). [The structure of probabilistic networks](#). *Methods in Ecology and Evolution*, 7, 303–312.

351 Poiset, T., Guéveneux-Julien, C., Fortin, M.-J., Gravel, D. & Legendre, P. (2017). [Hosts, parasites and their](#)
352 [interactions respond to different climatic variables](#). *Global Ecology and Biogeography*, 26, 942–951.

353 Poiset, T., Stouffer, D.B. & Gravel, D. (2015). [Beyond species: Why ecological interaction networks vary](#)
354 [through space and time](#). *Oikos*, 124, 243–251.

355 Saravia, L.A., Marina, T.I., Kristensen, N.P., De Troch, M. & Momo, F.R. (2022). [Ecological network](#)
356 [assembly: How the regional metaweb influences local food webs](#). *Journal of Animal Ecology*, n/a.

357 Statistics Canada. (2022). *Boundary files, reference guide second edition, Census year 2021*. Second edition.
358 Statistics Canada = Statistique Canada, Ottawa.

359 Strydom, T., Bouskila, S., Banville, F., Barros, C., Caron, D., Farrell, M.J., *et al.* (2022a). [Food web](#)
360 [reconstruction through phylogenetic transfer of low-rank network representation](#). *Methods in Ecology and*
361 *Evolution*, n/a.

362 Strydom, T., Bouskila, S., Banville, F., Barros, C., Caron, D., Farrell, M.J., *et al.* (2022b). [Predicting metawebs:](#)
363 [Transfer of graph embeddings can help alleviate spatial data deficiencies](#).

364 Strydom, T., Catchen, M.D., Banville, F., Caron, D., Dansereau, G., Desjardins-Proulx, P., *et al.* (2021). [A](#)
365 [roadmap towards predicting species interaction networks \(across space and time\)](#). *Philosophical*
366 *Transactions of the Royal Society B: Biological Sciences*, 376, 20210063.

367 Tuanmu, M.-N. & Jetz, W. (2014). [A global 1-km consensus land-cover product for biodiversity and ecosystem](#)
368 [modelling](#). *Global Ecology and Biogeography*, 23, 1031–1045.

369 Vasconcelos, T.S., Nascimento, B.T.M. do & Prado, V.H.M. (2018). [Expected impacts of climate change](#)
370 [threaten the anuran diversity in the Brazilian hotspots](#). *Ecology and Evolution*, 8, 7894–7906.

371 Wisz, M.S., Pottier, J., Kissling, W.D., Pellissier, L., Lenoir, J., Damgaard, C.F., *et al.* (2013). [The role of biotic](#)
372 [interactions in shaping distributions and realised assemblages of species: Implications for species](#)
373 [distribution modelling](#). *Biological Reviews*, 88, 15–30.

374 Youden, W.J. (1950). [Index for rating diagnostic tests](#). *Cancer*, 3, 32–35.

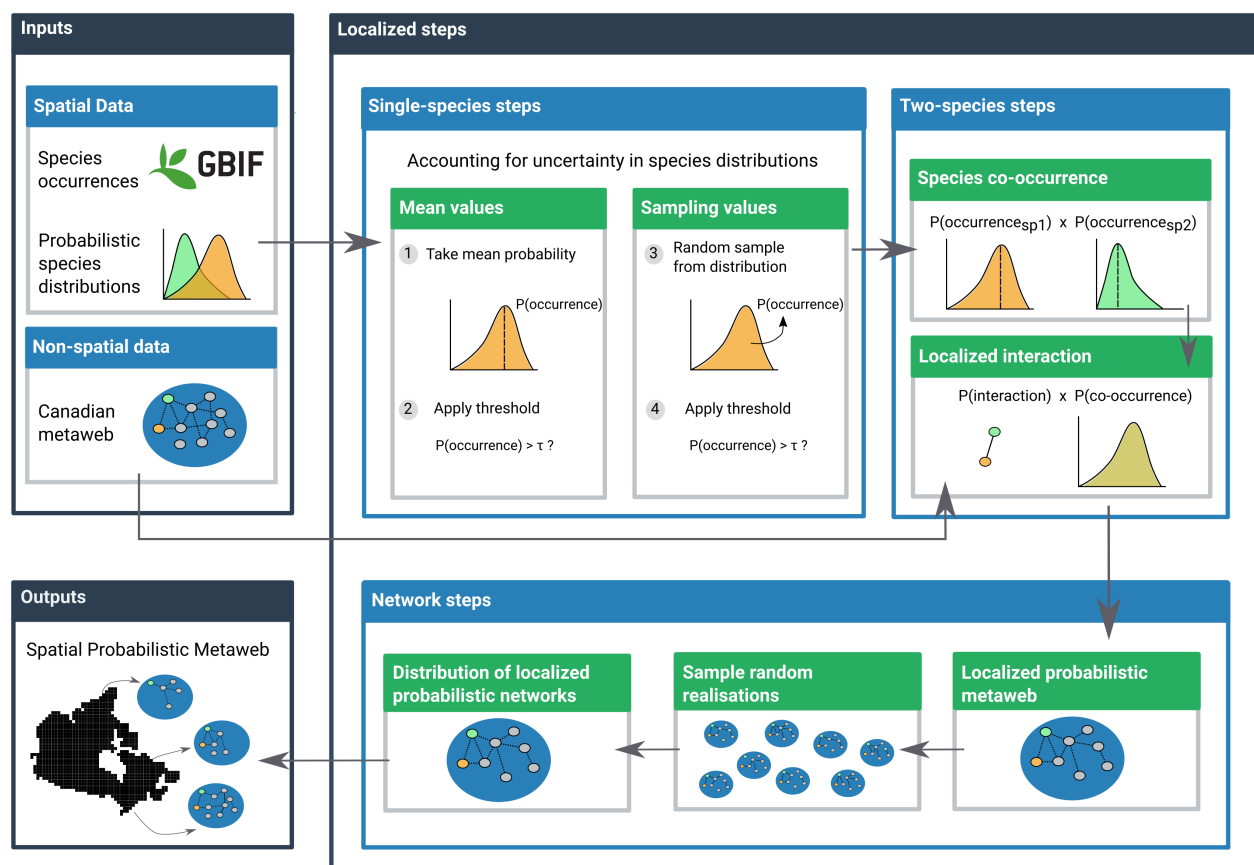


Figure 1: Conceptual figure of the workflow to obtain the spatial probabilistic metaweb (Chapter 1). The workflow has three components: the inputs, the localized steps, and the final spatial output. The inputs are composed of the spatial data (data with information in every cell) and the non-spatial data (constant for all of Canada). The localized steps use these data and are performed separately in every cell, first at a single-species level (using distribution data), then for every species pair (adding interaction data from the metaweb), and finally at the network level by combining the results of all species pairs. The final output coming out of the network-level steps contains a spatialized probabilistic metaweb for every cell across the study extent.

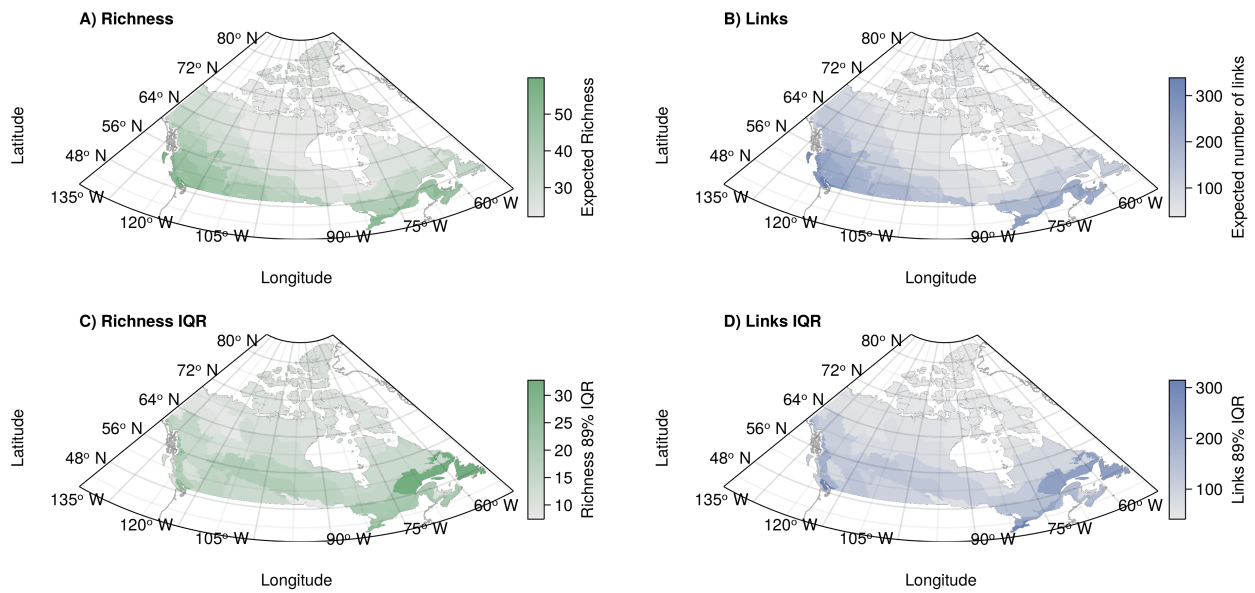


Figure 2: (A-B) Example of a community measure (A, expected species richness) and a network one (B, expected number of links). Both measures are assembled from the predicted probabilistic communities and networks, respectively. Values are first measured separately for all sites, then the median value is taken to represent the ecoregion-level value. (C-B) Representation of the 89% interquantile range of values within the ecoregion for expected richness (C) and expected number of links (D).

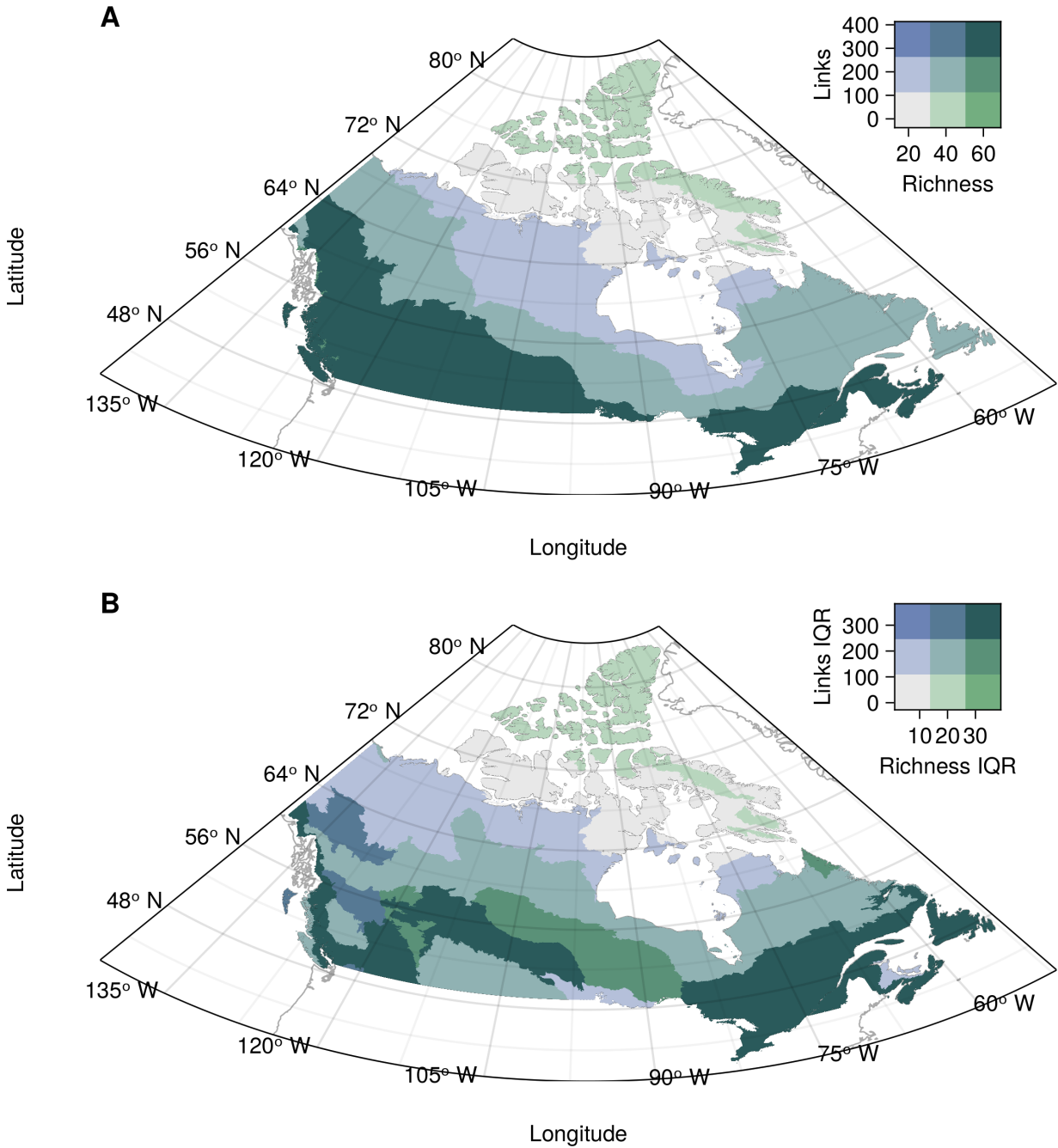


Figure 3: Bivariate relationship between community and network measures for the median ecoregion value (A) and the within-ecoregion 89% interquantile range (B). Values are grouped into three quantiles separately for each variable. The colour combinations represent the nine possible combinations of quantiles. Species richness (horizontal axis) goes left to right from low (light grey, bottom left) to high (green, bottom right). The number of links goes bottom-up from low (light grey, bottom left) to high (blue, top left).

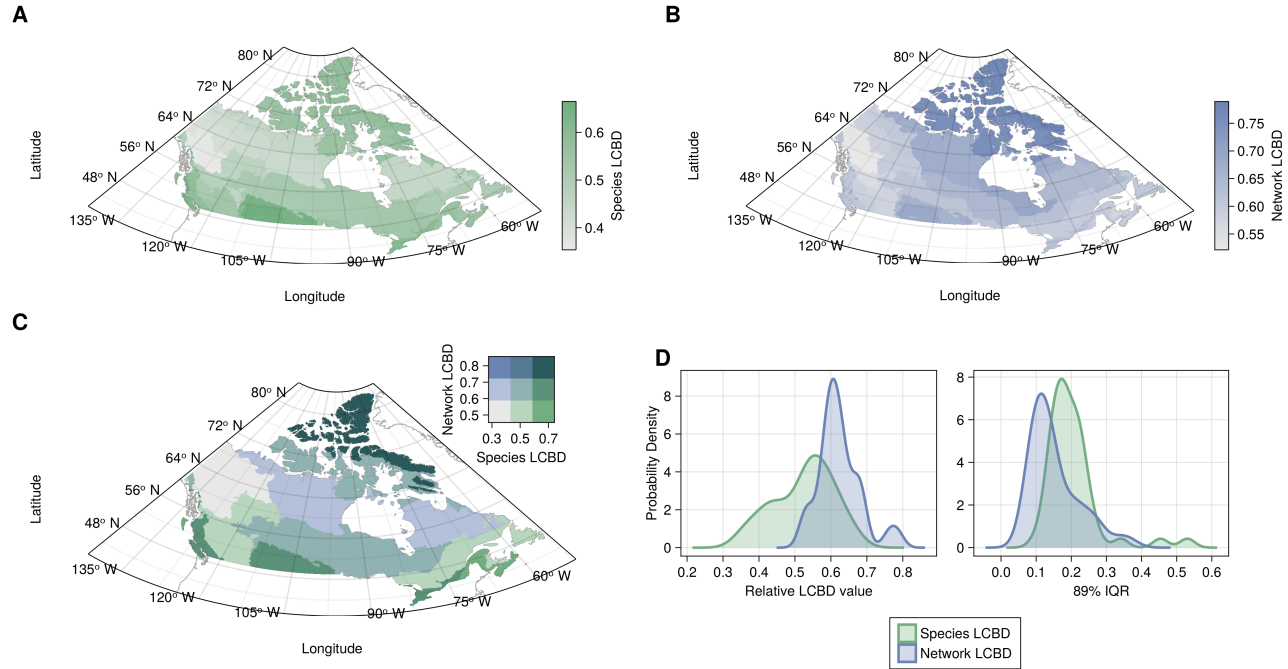


Figure 4: (A-B) Representation of the ecoregion uniqueness values based on species composition (a) and network composition (b). LCBD values were first computed across all sites and scaled relative to the maximum value observed. The ecoregion LCBD value is the median value for the sites in the ecoregion. (C) Bivariate representation of species and network composition LCBD. Values are grouped into three quantiles separately for each variable. The colour combinations represent the nine possible combinations of quantiles. The species uniqueness (horizontal axis) goes left to right from low uniqueness (light grey, bottom left) to high uniqueness (green, bottom right). The network composition uniqueness goes bottom-up from low uniqueness (light grey, bottom left) to high uniqueness (blue, top left). (D) Probability densities for the ecoregion LCBD values for species and network LCBD (left), highlighting the variability of the LCBD between ecoregions, and the 89% interquartile range of the values within each ecoregion (right), highlighting the variability within the ecoregions.